ISWCS 2022

18th International Symposium on

Wireless Communication Systems (ISWCS'22)

Reconfigurable Intelligent Surface Assisted Localization over Near-Field Beam Squint Effect

Zhuoran Li, Ziwei Wan, Keke Ying, Yikun Mei, Malong Ke, and Zhen Gao

Beijing Institute of Technology (BIT), Beijing, China

lizhuoran@bit.edu.cn, gaozhen16@bit.edu.cn

July 20, 2023

北京理工大学 BEIJING INSTITUTE OF TECHNOLOGY

Contents

1. Introduction

1.1 Near-Field Beam Squint Effect

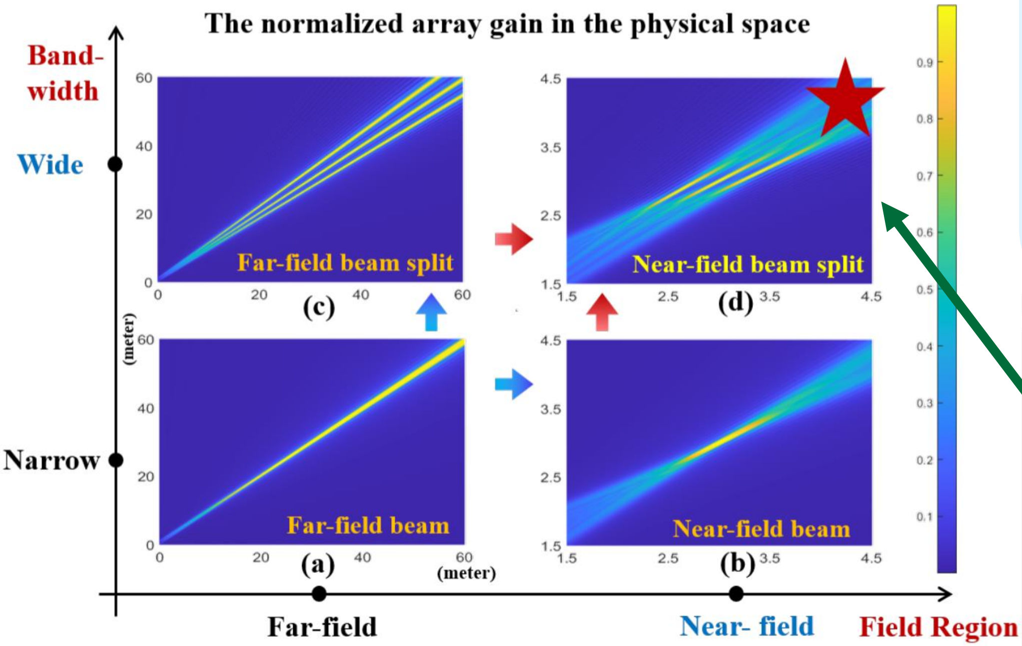

Fig. 1. This figure plots the normalized array gain in the physical space [Cui'21].

- XL-MIMO
  - The antenna aperture becomes larger.
- mmWave/THz
  - The carrier frequency and bandwidth become larger.

The large antenna aperture and carrier frequency result in the **large Rayleigh distance** [Cui'21].

The large bandwidth result in the **beam squint** effect [Liao'21].

[Liao'21] A. Liao, Z. Gao, D. Wang, H. Wang, H. Yin, D. W. K. Ng, and M.-S. Alouini, "Terahertz Ultra-Massive MIMO-Based Aeronautical Communications in Space-Air-Ground Integrated Networks," IEEE J. Sel. Areas Commun., vol. 39, no. 6, pp. 1741–1767, Jun. 2021.

[Cui'21] M. Cui, L. Dai, R. Schober, and L. Hanzo, "Near-Field Wideband Beamforming for Extremely Large Antenna Arrays," arXiv preprint arXiv: 2109.10054, 2021.

1. Introduction

1.2 General Localization Methods

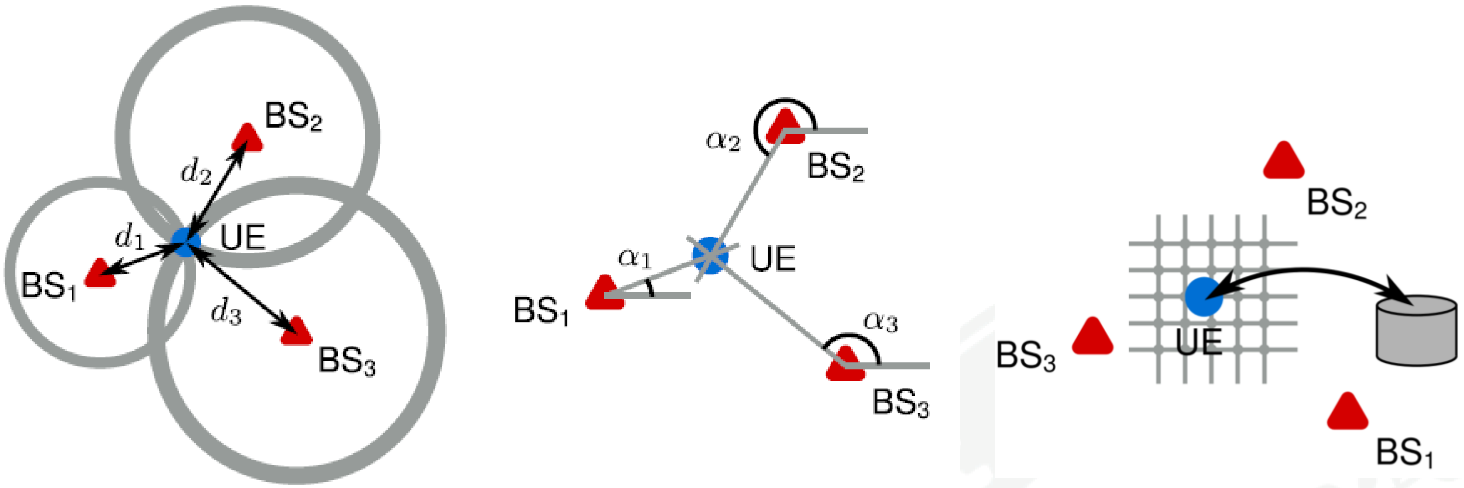

(a) Trilateration (b) Triangulation (c) Received Signal Strength

Fig. 2. General localization methods [Peral-Rosado'18].

- Trilateration
  - Time of Arrival (**ToA**),
  - Time Difference of Arrival (**TDoA**)
- Triangulation
  - Angle of Arrival (**AoA**)
- Received Signal Strength (**RSS**)
  - Mostly used indoors

[Peral-Rosado'18] J. A. del Peral-Rosado, R. Raulefs, J. A. López-Salcedo and G. Seco-Granados, "Survey of Cellular Mobile Radio Localization Methods: From 1G to 5G," in IEEE Communications Surveys & Tutorials, vol. 20, no. 2, pp. 1124-1148, Secondquarter 2018.

1.3 RIS-assisted Localization

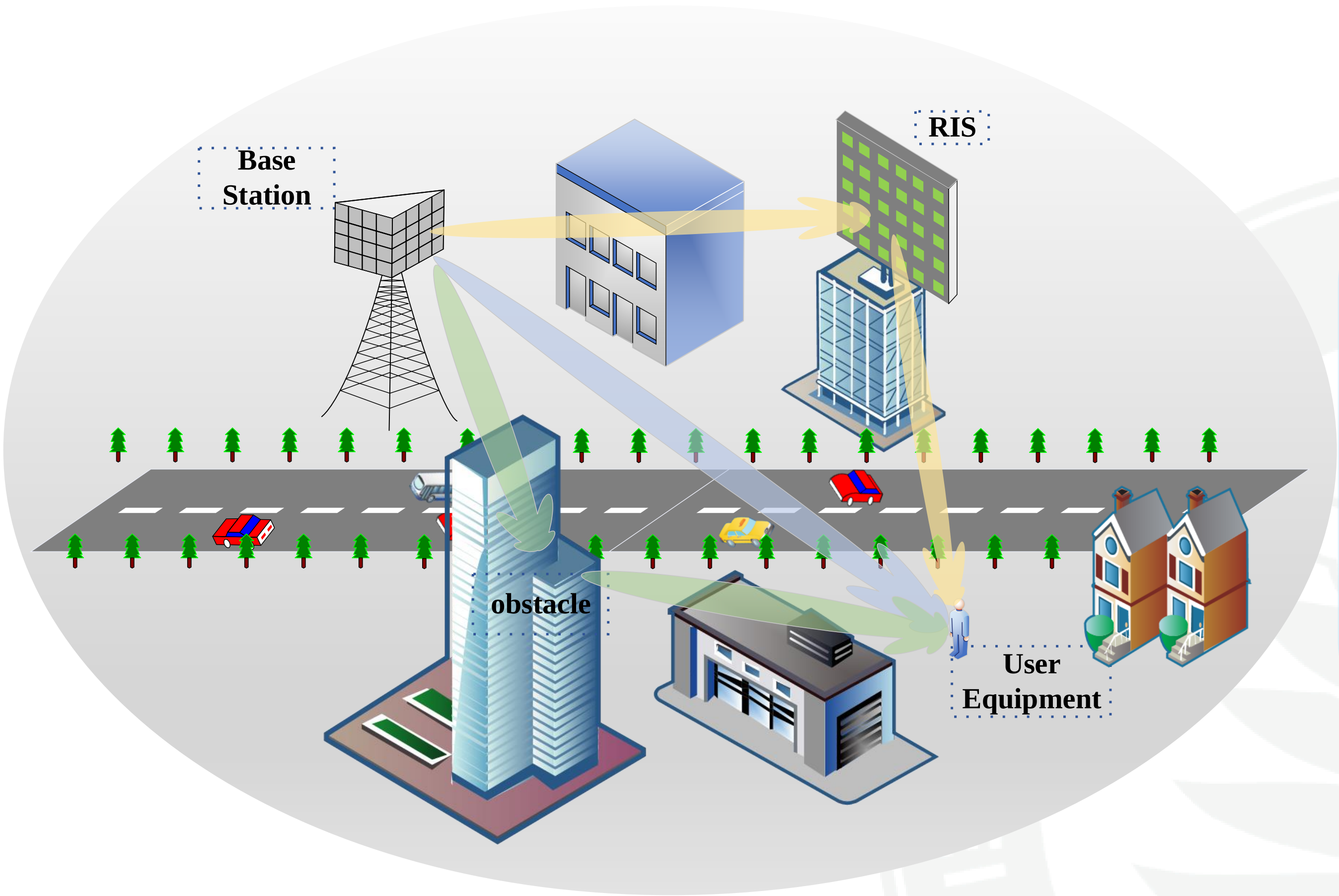

Fig. 3. RIS-assisted localization scenario.

- RIS can provide **additional** ToA and AoA observation degree of **freedom**.
- RIS can be densely deployed with **scalable** cost and **low** energy consumption [Wu'20].

[Wu'20] Q. Wu and R. Zhang, "Towards Smart and Reconfigurable Environment: Intelligent Reflecting Surface Aided Wireless Network," IEEE Commun. Mag., vol. 58, no. 1, pp. 106–112, Jan. 2020.

北京理工大学 BEIJING INSTITUTE OF TECHNOLOGY

Contents

2. System Model

- The received pilot **without the assistance** of the RIS in the m-th subcarrier and p-th time slot is denoted by $\mathbf{y}_{p,m}^{\text{NRIS}} \in \mathbb{C}^{N_{\text{RF}}\times 1}$, whose expression is

$$\mathbf{y}_{p,m}^{\text{NRIS}} = \mathbf{A}_{p}^{\text{NRIS}} \mathbf{h}_{:,m}^{\text{BU}} x_{p,m} + \mathbf{n}_{p,m}^{\text{NRIS}} \tag{1}$$

where $x_{p,m}$, $\mathbf{h}_{:,m}^{\text{BU}} \in \mathbb{C}^{N\times 1}$, and $\mathbf{A}_{p}^{\text{NRIS}} \in \mathbb{C}^{N_{\text{RF}}\times N}$ denote the pilot transmitted by the UE, the near-field channel between the BS and the UE, and the phase shift network (PSN) of the BS, respectively.

- Furthermore, the received pilot **with the assistance** of the RIS in the m-th subcarrier and p-th time slot is denoted by $\mathbf{y}_{p,m}^{\text{RIS}} \in \mathbb{C}^{N_{\text{RF}}\times 1}$, whose expression is

$$\mathbf{y}_{p,m}^{\text{RIS}} = \mathbf{A}_{p}^{\text{RIS}} \mathbf{H}_{:,:,m}^{\text{BR}} \mathbf{\Phi}_{p}^{\text{RIS}} \mathbf{h}_{:,m}^{\text{RU}} x_{p,m} + \mathbf{A}_{p}^{\text{RIS}} \mathbf{h}_{:,m}^{\text{BU}} x_{p,m} + \mathbf{n}_{p,m}^{\text{RIS}} \tag{2}$$

2. System Model

- We assume $x_{p,m}=1$, and **stack** the received P^{NRIS} pilots without the assistance of RIS as follows,

$$\mathbf{Y}_{:,m}^{\mathrm{NRIS}}=[(\mathbf{y}_{1,m}^{\mathrm{NRIS}})^T,\cdots,(\mathbf{y}_{P^{\mathrm{NRIS}},m}^{\mathrm{NRIS}})^T]^T \quad (3)$$

$$\bar{\mathbf{A}}^{\mathrm{NRIS}}=[(\mathbf{A}_1^{\mathrm{NRIS}})^T,\cdots,(\mathbf{A}_{P^{\mathrm{NRIS}}}^{\mathrm{NRIS}})^T]^T \quad (4)$$

$$\mathbf{N}_{:,m}^{\mathrm{NRIS}}=[(\mathbf{n}_{1,m}^{\mathrm{NRIS}})^T,\cdots,(\mathbf{n}_{P^{\mathrm{NRIS}},m}^{\mathrm{NRIS}})^T]^T \quad (5)$$

Therefore, we can obtain

$$\mathbf{Y}_{:,m}^{\mathrm{NRIS}}=\bar{\mathbf{A}}^{\mathrm{NRIS}}\mathbf{h}_{:,m}^{\mathrm{BU}}+\mathbf{N}_{:,m}^{\mathrm{NRIS}} \quad (6)$$

- Similarly, we have

$$\mathbf{Y}_{:,m}^{\mathrm{RIS}}=\bar{\mathbf{A}}_{:,:,m}^{\mathrm{RIS}}\mathbf{h}_{:,m}^{\mathrm{RU}}+\bar{\mathbf{A}}_{:,:,m}^{\mathrm{RIS}}\mathbf{h}_{:,m}^{\mathrm{BU}}+\mathbf{N}_{:,m}^{\mathrm{RIS}} \quad (7)$$

where

$$\bar{\mathbf{A}}_{:,:,m}^{\mathrm{RIS}}=[(\mathbf{A}_1^{\mathrm{RIS}}\mathbf{H}_{:,:,m}^{\mathrm{BR}}\mathbf{\Phi}_1^{\mathrm{RIS}})^T,\cdots,(\mathbf{A}_{P^{\mathrm{RIS}}}^{\mathrm{RIS}}\mathbf{H}_{:,:,m}^{\mathrm{BR}}\mathbf{\Phi}_{P^{\mathrm{RIS}}}^{\mathrm{RIS}})^T]^T \quad (8)$$

2. System Model

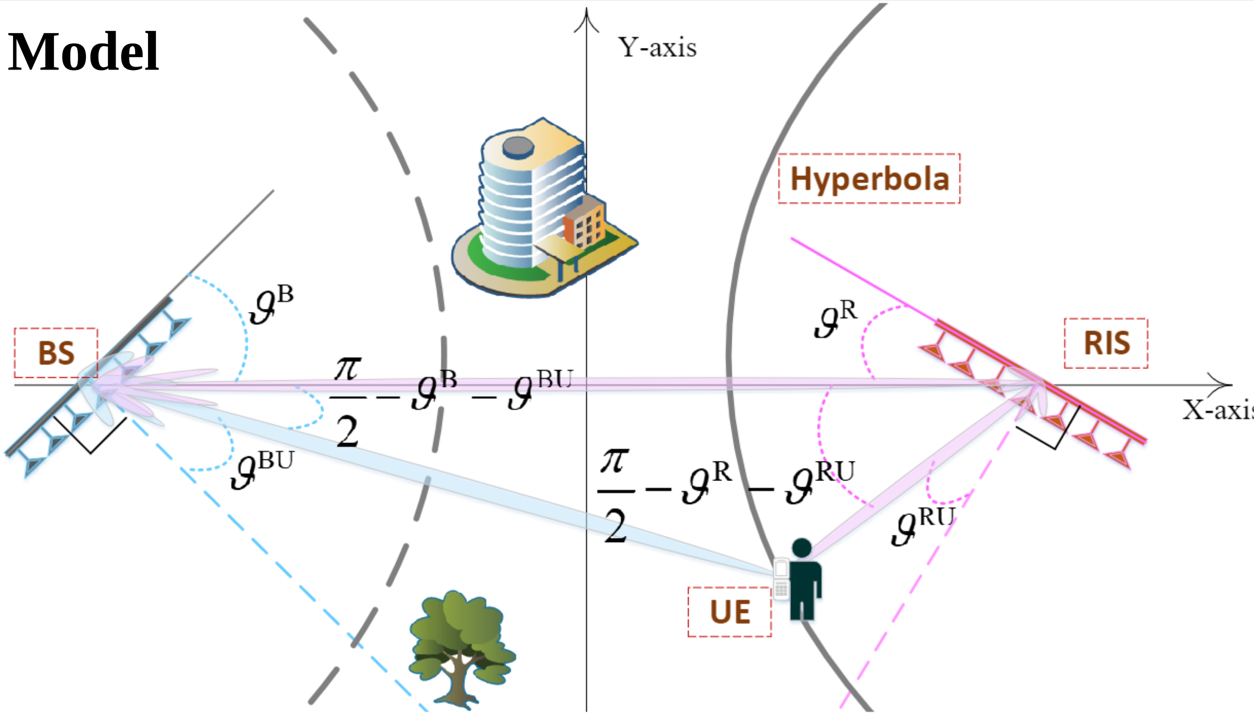

Fig. 4. The model of a RIS-assisted localization system

- the **near-field channel** can be modeled as follows[Cui'22]

$$\mathbf{h}_{:,m}^{BU} = \sum_{l=0}^{L} \alpha_{l,m}^{BU} e^{-jk_m r_l^{BU}} \mathbf{b}_{m,l}^{BU}(f_m, \theta_l^{BU}, r_l^{BU}) \tag{9}$$

- The **near-field steering vector** can be acquired as

$$\mathbf{b}_{m,l}^{BU}(f_m, \theta_l^{BU}, r_l^{BU}) = \frac{1}{\sqrt{N}}[e^{-jk_m(r_{l,0}^{BU}-r_l^{BU})}, \cdots, e^{-jk_m(r_{l,N-1}^{BU}-r_l^{BU})}]^T \tag{10}$$

[Cui'22] M. Cui and L. Dai, "Channel Estimation for Extremely Large-Scale MIMO: Far-Field or Near-Field?" IEEE Trans. Commun., vol. 70, no. 4, pp. 2663–2677, Apr. 2022.

Contents

3.1 Correlation of dictionary under the Near-Field Beam Squint Effect

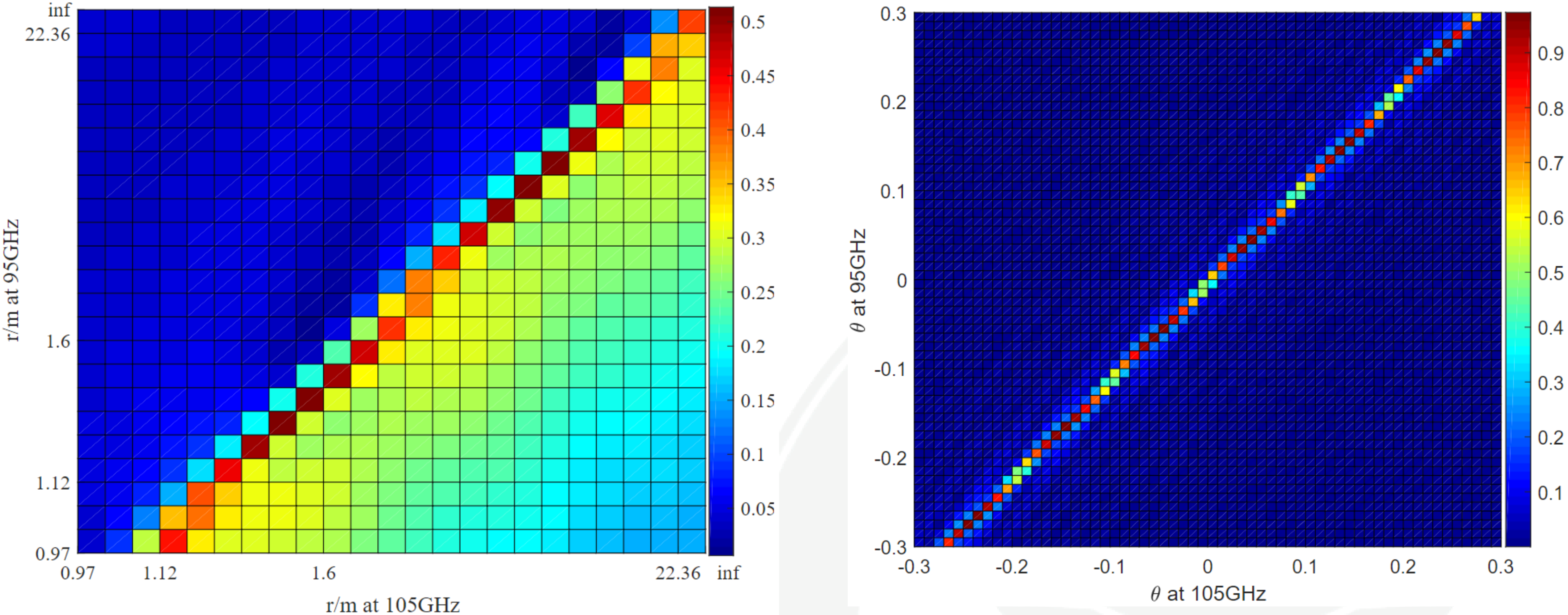

(a) correlation of the near-field steering vectors at different frequencies and different distances.

(b) correlation of the near-field steering vectors at different frequencies and different AoAs.

Fig. 5. The near-field beam squint effect can be observed by the **correlation of the steering vectors**.

3. Proposed RIS-assisted localization solution

3.2 RIS-assisted localization (RISAL) algorithm

The process of the RISAL algorithm

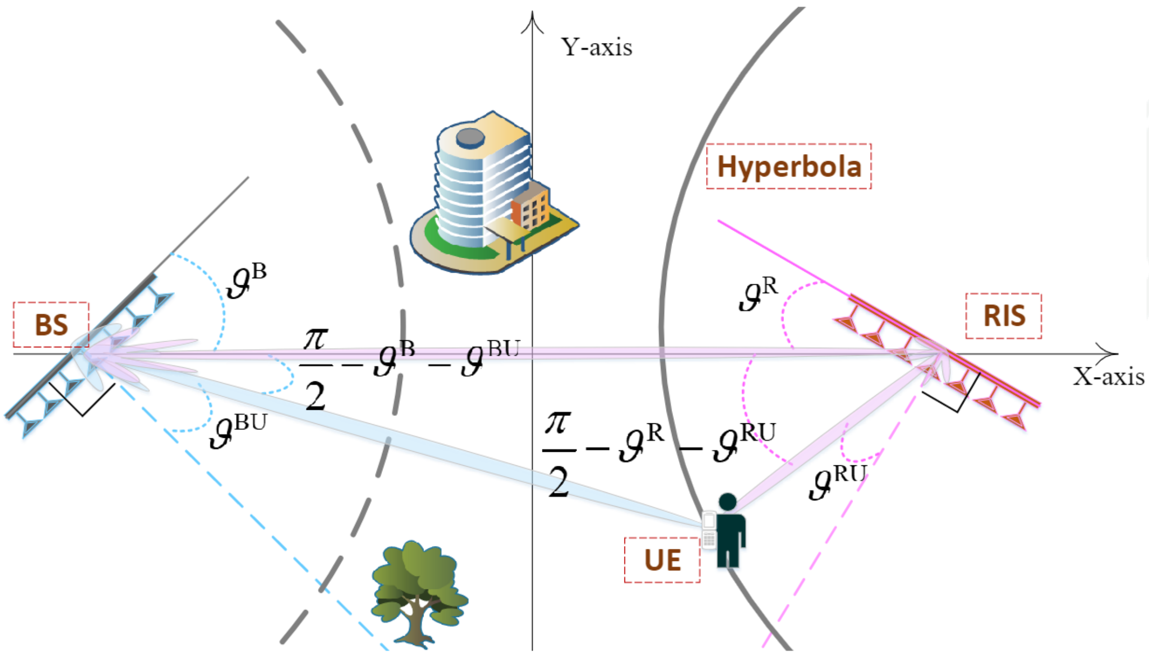

Fig. 6. The model of a RIS-assisted localization system

Algorithm 1: The Proposed RISAL Algorithm

Input: $\mathbf{Y}^{\mathrm{NRIS}} \in \mathbb{C}^{N_{\mathrm{RF}} \cdot P^{\mathrm{NRIS}} \times M}$, $\mathbf{Y}^{\mathrm{RIS}} \in \mathbb{C}^{N_{\mathrm{RF}} \cdot P^{\mathrm{RIS}} \times M}$, $\bar{\mathbf{A}}^{\mathrm{NRIS}} \in \mathbb{C}^{N_{\mathrm{RF}} \cdot P^{\mathrm{NRIS}} \times N}$, $I_{\max}$, $\bar{\mathbf{A}}^{\mathrm{RIS}} \in \mathbb{C}^{N_{\mathrm{RF}} \cdot P^{\mathrm{RIS}} \times N_{\mathrm{RIS}} \times M}$

Output: $r_{\mathrm{UE}}^{\mathrm{fi}}$, $\theta_{\mathrm{UE}}^{\mathrm{fi}}$

1 Do spectral decomposition of $(\mathbf{Y}^{\mathrm{NRIS}})^H \mathbf{Y}^{\mathrm{NRIS}}$ and $(\mathbf{Y}^{\mathrm{RIS}})^H \mathbf{Y}^{\mathrm{RIS}}$ to obtain the matrices $\mathbf{E}^{\mathrm{NRIS}}$ and $\mathbf{E}^{\mathrm{RIS}}$ composed of eigenvectors as (7);
2 Obtain the noise subspaces $\bar{\mathbf{E}}^{\mathrm{NRIS}}$ and $\bar{\mathbf{E}}^{\mathrm{RIS}}$ as (8);
3 Obtain the two kinds of delays $\tau_{\mathrm{est}}^{\mathrm{NRIS}}$ and $\tau_{\mathrm{est}}^{\mathrm{RIS}}$ as (9);
4 Obtain the τ_{TDoA} as (10) and the hyperbola equation as (11);
5 Generate polar-domain dictionary $\mathbf{W}^{\mathrm{h}}$ as [2] on the hyperbola and obtain the coarse estimation $\theta_{\mathrm{BS}}^{\mathrm{co}}$ by the correlation as (12);
6 Combine the hyperbola and $\theta_{\mathrm{UE}}^{\mathrm{co}}$ with the position of the BS, $(x_{\mathrm{BS}}, y_{\mathrm{BS}})$, to obtain $r_{\mathrm{UE}}^{\mathrm{co}}$ using (13) and (14);
7 Obtain $\bar{\mathbf{Y}}_{i,m}^{\mathrm{NRIS}}$ as (17);
8 Obtain the loss function v^{NRIS} without the assistance of the RIS as (18);
9 $\theta_{\mathrm{UE}}^{\mathrm{it}} = \theta_{\mathrm{UE}}^{\mathrm{co}}$;
10 **while** *iteration* $< I_{max}$ **do**
11   Substitute $(\theta_{\mathrm{UE}}^{\mathrm{it}}, r_{\mathrm{UE}}^{\mathrm{co}})$ into $(\hat{\theta}_0^{\mathrm{BU}}, \hat{r}_0^{\mathrm{BU}})$ and then obtain the $\nabla = \frac{\partial v^{\mathrm{NRIS}}}{\partial \hat{\theta}_0^{\mathrm{BU}}}$ as (20);
12   Use Armijo-Goldstein rule to update the step Δ based on the ∇ and $\theta_{\mathrm{UE}}^{\mathrm{it}}$;
13   Update the $\theta_{\mathrm{UE}}^{\mathrm{it}}$ as $\theta_{\mathrm{UE}}^{\mathrm{it}} = \theta_{\mathrm{UE}}^{\mathrm{it}} - \Delta \cdot \nabla$;
14 **end**
15 $\theta_{\mathrm{UE}}^{\mathrm{fi}} = \theta_{\mathrm{UE}}^{\mathrm{it}}$. Then combine the hyperbola and $\theta_{\mathrm{UE}}^{\mathrm{fi}}$ with the position of the BS, $(x_{\mathrm{BS}}, y_{\mathrm{BS}})$, to obtain $r_{\mathrm{UE}}^{\mathrm{fi}}$ using (13) and (14) and return $r_{\mathrm{UE}}^{\mathrm{fi}}$, $\theta_{\mathrm{UE}}^{\mathrm{fi}}$;

3.2 RIS-assisted localization (RISAL) algorithm

Obtain the coarse UE location using TDoA

- We utilize the $\mathbf{Y}^{\text{NRIS}}$ and $\mathbf{Y}^{\text{RIS}}$ to do **spectral decomposition** as

$$(\mathbf{Y}^{\text{NRIS}})^H \mathbf{Y}^{\text{NRIS}} = \mathbf{E}^{\text{NRIS}} \Lambda^{\text{NRIS}} (\mathbf{E}^{\text{NRIS}})^{\text{H}} \tag{11a}$$

$$(\mathbf{Y}^{\text{RIS}})^H \mathbf{Y}^{\text{RIS}} = \mathbf{E}^{\text{RIS}} \Lambda^{\text{RIS}} (\mathbf{E}^{\text{RIS}})^{\text{H}} \tag{11b}$$

- And we treat the eigenvectors corresponding to all but the largest eigenvalues as the **noise subspaces** as

$$\overline{\mathbf{E}}^{\text{NRIS}} = \mathbf{E}^{\text{NRIS}}_{:,2:\text{end}} \tag{12a}$$

$$\overline{\mathbf{E}}^{\text{RIS}} = \mathbf{E}^{\text{RIS}}_{:,2:\text{end}} \tag{12b}$$

- $\tau^{\text{NRIS}}_{\text{est}}$, the delay from the UE to the BS directly, and $\tau^{\text{RIS}}_{\text{est}}$, the delay from the UE to the BS via the RIS, can be calculated as

$$\tau^{\text{NRIS}}_{\text{est}} = \arg\max_{\tau}\left(\frac{1}{\mathbf{a}(\tau)\cdot\overline{\mathbf{E}}^{\text{NRIS}}\cdot(\mathbf{a}(\tau)\cdot\overline{\mathbf{E}}^{\text{NRIS}})^H}\right) \tag{13a}$$

$$\tau^{\text{RIS}}_{\text{est}} = \arg\max_{\tau}\left(\frac{1}{\mathbf{a}(\tau)\cdot\overline{\mathbf{E}}^{\text{RIS}}\cdot(\mathbf{a}(\tau)\cdot\overline{\mathbf{E}}^{\text{RIS}})^H}\right) \tag{13b}$$

where $\mathbf{f} \in \mathbb{C}^{1\times M}$ is the frequency vector in M subcarriers and $\mathbf{a}(\tau) = e^{j\tau\mathbf{f}} \in \mathbb{C}^{1\times M}$.

3. Proposed RIS-assisted localization solution

3.2 RIS-assisted localization (RISAL) algorithm

Obtain the coarse UE location using TDoA

- We obtain the **time difference** between the UE arriving at the BS and the UE arriving at the RIS as

$$\tau_{\text{TDoA}} = \tau_{\text{est}}^{\text{NRIS}} - (\tau_{\text{est}}^{\text{RIS}} - \frac{r_{\text{B2R}}}{c}) \tag{14}$$

- Then we can acquire the standard equation of the **hyperbola** to lock the UE on it

$$\frac{x^2}{a_{\text{h}}^2} - \frac{y^2}{b_{\text{h}}^2} = 1 \tag{15}$$

where $a_{\text{h}} = \frac{\tau_{\text{TDoA}} \cdot c}{2}$ and $b_{\text{h}} = c_{\text{h}}^2 - a_{\text{h}}^2 = (\frac{r_{\text{B2R}}}{2})^2 - a_{\text{h}}^2$.

- Next we can obtain the **coarse AoA** from the UE to the BS by the correlation as

$$\theta_{\text{UE}}^{\text{co}} = \arg\max_{\theta} \sum_{m=1}^{M} (\bar{\mathbf{A}}^{\text{NRIS}} \mathbf{W}_{:,:,m}^{\text{h}}(\theta))^H \mathbf{Y}_{:,m}^{\text{NRIS}} \tag{16}$$

- By combining $\theta_{\text{UE}}^{\text{co}}$ with the position of the BS, denoted as $(x_{\text{BS}}, y_{\text{BS}})$, the **location of the UE** can be calculated as the intersection of the line and the hyperbola

$$x_{\text{UE}}^{\text{co}} = \frac{\sqrt{4k^4a^4x_{\text{BS}}^2 + 4a^2(b^2 - a^2k^2)(k^2x_{\text{BS}}^2 + b^2)}}{2(b^2 - a^2k^2)} + \frac{-2a^2k^2x_{\text{BS}}}{2(b^2 - a^2k^2)} \tag{17}$$

$$y_{\text{UE}}^{\text{co}} = k(x_{\text{UE}}^{\text{co}} - x_{\text{BS}})$$

3. Proposed RIS-assisted localization solution

3.2 RIS-assisted localization (RISAL) algorithm

Refine the UE location: the problem of conventional loss function

- The **conventional** loss function[2][16]

$$v^{\mathrm{NRIS}} = \sum_{m=1}^{M} \left\| \mathbf{Y}_{:,m}^{\mathrm{NRIS}} - \bar{\mathbf{A}}^{\mathrm{NRIS}} \mathbf{h}_{:,m}^{\mathrm{BU}} \right\|_{\mathrm{F}}^{2} \quad (18)$$

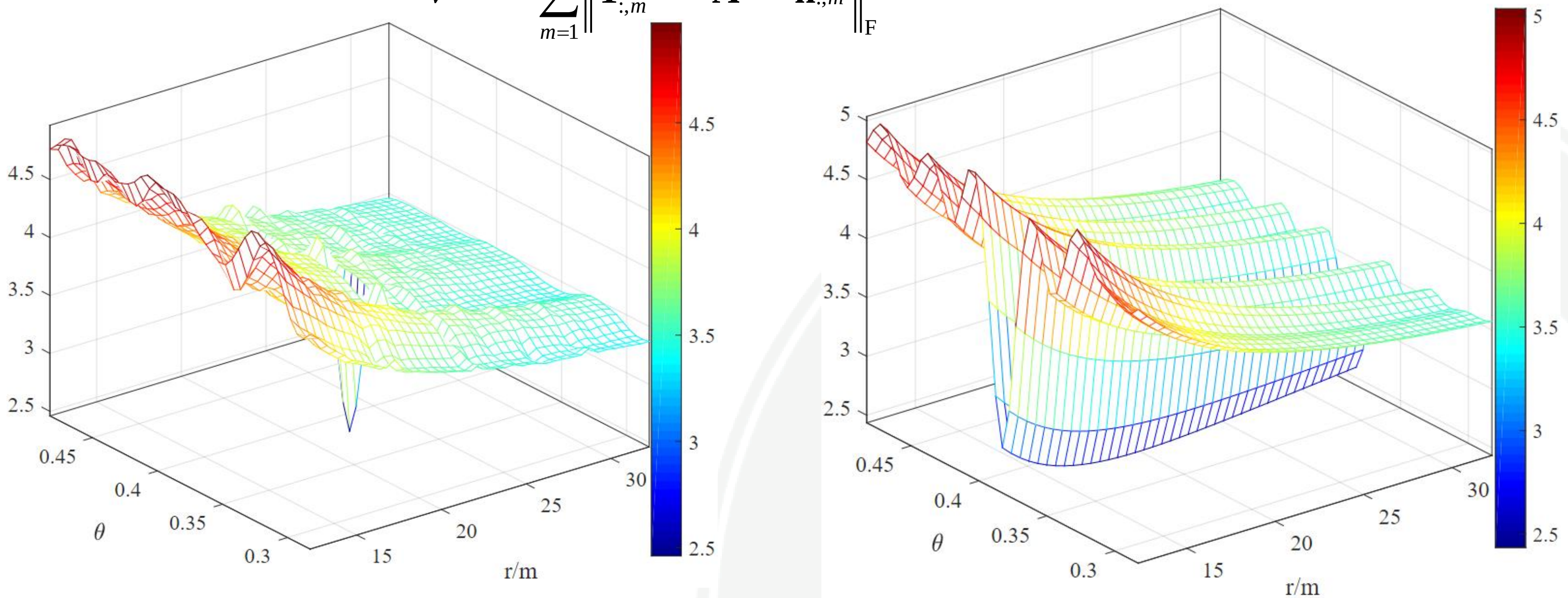

(a) (b)

Fig. 7. The view of the absolute value of the loss function when signal to noise ratio (SNR) is 0dB. (a) The loss function is the conventional one. (b) The loss function is the proposed one.

- **Proposed** loss function

$$v^{\mathrm{NRIS}} = \sum_{m=1}^{M} \left\| \bar{\mathbf{Y}}_{:,m}^{\mathrm{NRIS}} - \bar{\mathbf{A}}^{\mathrm{NRIS}} \bar{\mathbf{h}}_{:,m}^{\mathrm{BU}} \right\|_{\mathrm{F}}^{2} = \left\| \bar{\mathbf{Y}}^{\mathrm{NRIS}} - \bar{\mathbf{A}}^{\mathrm{NRIS}} \bar{\mathbf{h}}^{\mathrm{BU}} \right\|_{\mathrm{F}}^{2} \quad (19)$$

3.2 RIS-assisted localization (RISAL) algorithm

Refine the UE location: how to acquire the proposed loss function

- Let the PSN of the first RF-chain in one of all time slots, namely $\bar{\mathbf{A}}_{1,:}^{\mathrm{NRIS}}$, to be

$$\begin{cases} \underbrace{0 \ \cdots \ 0}_{\frac{N-1}{2}} \ 1 \ \underbrace{0 \ \cdots \ 0}_{\frac{N-1}{2}}, \text{ if } N \text{ is odd} \\ \underbrace{0 \ \cdots \ 0}_{\frac{N-2}{2}} \ 1 \ 1 \ \underbrace{0 \ \cdots \ 0}_{\frac{N-2}{2}}, \text{ if } N \text{ is even} \end{cases} \quad (20)$$

- The **imaginary LoS channel** can be expressed as

$$\bar{\mathbf{h}}_{:,m}^{\mathrm{BU}} = \hat{\alpha}_{0,m}^{\mathrm{BU}} \mathbf{b}_{m,0}^{\mathrm{BU}} (f_m, \hat{\theta}_0^{\mathrm{BU}}, \hat{r}_0^{\mathrm{BU}}) \quad (21)$$

where $\hat{\alpha}_{0,m}^{\mathrm{BU}}$, $\hat{r}_0^{\mathrm{BU}}$ and $\hat{\theta}_0^{\mathrm{BU}}$ denotes the estimated channel gain, the estimated distance, and the estimated AoA, respectively.

- The **imaginary received signal** can be calculated as

$$\begin{cases} \bar{\mathbf{Y}}_{i,m}^{\mathrm{NRIS}} = \mathbf{Y}_{i,m}^{\mathrm{NRIS}}, \text{ for } i = 1 \\ \bar{\mathbf{Y}}_{i,m}^{\mathrm{NRIS}} = \mathbf{S}_{i,m} \dfrac{\sqrt{\sum_{m=1}^{M} | \mathbf{Y}_{i,m}^{\mathrm{NRIS}} |^2}}{\sqrt{\sum_{m=1}^{M} | \mathbf{S}_{i,m} |^2}}, \text{ for } i = 2, \cdots, N_{\mathrm{RF}} P^{\mathrm{NRIS}} \end{cases} \quad (22)$$

where $\mathbf{S}_{i,m} = \mathbf{Y}_{i,m}^{\mathrm{NRIS}} / \mathbf{Y}_{1,m}^{\mathrm{NRIS}}$.

~~$e^{-jk_m r_l^{\mathrm{BU}}}$ in (9)~~

3.2 RIS-assisted localization (RISAL) algorithm

Refine the UE location: the polar-domain gradient descent algorithm

- Get the **proposed loss function** from the imaginary received signal and the imaginary LoS channel as follows

$$v^{\mathrm{NRIS}} = \sum_{m=1}^{M} \left\| \bar{\mathbf{Y}}^{\mathrm{NRIS}}_{:,m} - \bar{\mathbf{A}}^{\mathrm{NRIS}} \bar{\mathbf{h}}^{\mathrm{BU}}_{:,m} \right\|_{\mathrm{F}}^{2} = \left\| \bar{\mathbf{Y}}^{\mathrm{NRIS}} - \bar{\mathbf{A}}^{\mathrm{NRIS}} \bar{\mathbf{h}}^{\mathrm{BU}} \right\|_{\mathrm{F}}^{2} \tag{23}$$

- The **gradient** of v^{NRIS} with respect to $\hat{\theta}_0^{\mathrm{BU}}$ is

$$\frac{\partial v^{\mathrm{NRIS}}}{\partial \hat{\theta}_0^{\mathrm{BU}}} = -2 \cdot \mathrm{Re}\{\mathrm{tr}[(\bar{\mathbf{A}}^{\mathrm{NRIS}} \frac{\partial \bar{\mathbf{h}}^{\mathrm{BU}}}{\partial \hat{\theta}_0^{\mathrm{BU}}})^H \bar{\mathbf{Y}}^{\mathrm{NRIS}}]\} + 2 \cdot \mathrm{Re}\{(\bar{\mathbf{A}}^{\mathrm{NRIS}} \bar{\mathbf{h}}^{\mathrm{BU}})^H \bar{\mathbf{A}}^{\mathrm{NRIS}} \frac{\partial \bar{\mathbf{h}}^{\mathrm{BU}}}{\partial \hat{\theta}_0^{\mathrm{BU}}}\} \tag{24}$$

- Besides, the **gradient** of the n-th element of $\bar{\mathbf{h}}^{\mathrm{BU}}_{:,m}$ with respect to $\hat{\theta}_0^{\mathrm{BU}}$ is derived as

$$\left.\frac{\partial \bar{\mathbf{h}}^{\mathrm{BU}}_{:,m}}{\partial \hat{\theta}_0^{\mathrm{BU}}}\right|_n = \beta \cdot \frac{\hat{r}_0^{\mathrm{BU}} \boldsymbol{\delta}_n d}{\sqrt{(\hat{r}_0^{\mathrm{BU}})^2 + \boldsymbol{\delta}_n^2 d^2 - 2\hat{r}_0^{\mathrm{BU}} \hat{\theta}_0^{\mathrm{BU}} \boldsymbol{\delta}_n d}} \tag{25}$$

- $\hat{\theta}_0^{\mathrm{BU}}$ is optimized by **gradient descent** and the derivation in the process of gradient descent is based on the above two equations.

  By the way, the step size is updated using Armijo-Goldstein rule.

- The overall steps of polar-domain gradient descent algorithm are summarized in step 7-14 in **Algorithm 1**: RISAL.

北京理工大学 BEIJING INSTITUTE OF TECHNOLOGY

Contents

4. Simulation Results

- Simulation parameters

TABLE I. Simulation parameters

Var.	Description	Value
N	No. of BS antenna	256
N_{RIS}	No. of RIS elements	256
N_{RF}	No. of RF-chain	4
$P^{\mathrm{NRIS}}/P^{\mathrm{RIS}}$	No. of time slots	8/16
f_c	Carrier frequency	0.1THz
B	Bandwidth	10GHz
M	No. of subcarriers	2048

- Root mean square error (RMSE) is the accuracy evaluation

$$\mathrm{RMSE}_{\vartheta}=\sqrt{\frac{\sum_{n=1}^{N_{\mathrm{it}}}(\hat{\vartheta}_n-\vartheta_{\mathrm{real}})^2}{N_{\mathrm{it}}}},\mathrm{RMSE}_{r}=\sqrt{\frac{\sum_{n=1}^{N_{\mathrm{it}}}(\hat{r}_n-r_{\mathrm{real}})^2}{N_{\mathrm{it}}}} \quad (26)$$

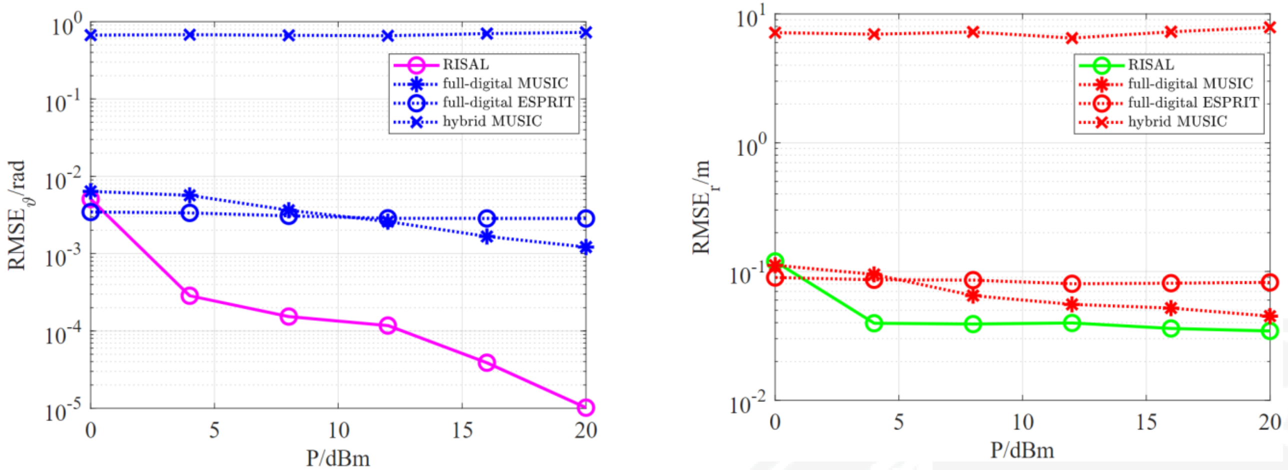

(a) RMSE_ϑ (b) RMSE_r

Fig. 8. RMSE performance of ϑ and r versus the transmit power under the **near-field beam squint effect**.

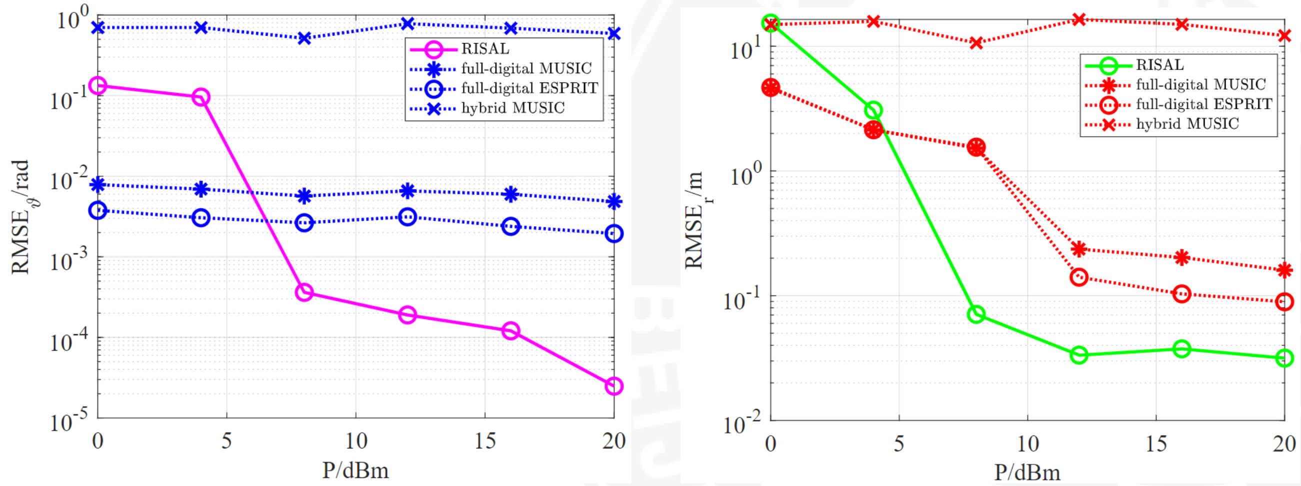

(a) RMSE_ϑ (b) RMSE_r

Fig. 9. RMSE performance of ϑ and r versus the transmit power in the **far-field** conditions with the beam squint effect.

北京理工大学 BEIJING INSTITUTE OF TECHNOLOGY

Contents

5. Conclusions

Contribution

- Numerical results verified that the RISAL algorithm can achieve **10^{-4} rad** of the AoA accuracy and **centimeter-level** of the distance accuracy, which **outperformed** the MUSIC algorithm and the ESPRIT algorithm, under the near-field beam squint effect.

Limitation

- The **on-grid** method is used to estimate the TDoA in this paper, which limits the accuracy of the **distance estimation**.

Future Direction

- The high-precision localization can be utilized in other important applications, such as assistance to communications, **combination with channel estimation**, etc.

Contents

6. References

[1] Z. Gao, L. Dai, Z. Wang, and S. Chen, “Spatially Common Sparsity Based Adaptive Channel Estimation and Feedback for FDD Massive MIMO,” IEEE Trans. Signal Process., vol. 63, no. 23, pp. 6169–6183, Dec. 2015.

[2] M. Cui and L. Dai, “Channel Estimation for Extremely Large-Scale MIMO: Far-Field or Near-Field?” IEEE Trans. Commun., vol. 70, no. 4, pp. 2663–2677, Apr. 2022.

[3] D. L. et al., “Convergent Communication, Sensing and Localization in 6G Systems: An Overview of Technologies, Opportunities and Challenges,” IEEE Access, vol. 9, pp. 26 902–26 925, 2021.

[4] Q. Wu and R. Zhang, “Towards Smart and Reconfigurable Environment: Intelligent Reflecting Surface Aided Wireless Network,” IEEE Commun. Mag., vol. 58, no. 1, pp. 106–112, Jan. 2020.

[5] A. Liao, Z. Gao, D. Wang, H. Wang, H. Yin, D. W. K. Ng, and M.-S. Alouini, “Terahertz Ultra-Massive MIMO-Based Aeronautical Communications in Space-Air-Ground Integrated Networks,” IEEE J. Sel. Areas Commun., vol. 39, no. 6, pp. 1741–1767, Jun. 2021.

[6] F. Gao, B. Wang, C. Xing, J. An, and G. Y. Li, “Wideband Beamforming for Hybrid Massive MIMO Terahertz Communications,” IEEE J. Sel. Areas Commun., vol. 39, no. 6, pp. 1725–1740, Jun. 2021.

[7] J. A. del Peral-Rosado, R. Raulefs, J. A. L´opez-Salcedo, and G. SecoGranados, “Survey of Cellular Mobile Radio Localization Methods: From 1G to 5G,” IEEE Commun. Surv. Tutor., vol. 20, no. 2, pp. 1124– 1148, 2018.

[8] Z. Lin, T. Lv, and P. T. Mathiopoulos, “3-D Indoor Positioning for Millimeter-Wave Massive MIMO Systems,” IEEE Trans. Commun., vol. 66, no. 6, pp. 2472–2486, Jun. 2018.

6. References

[9] N. Garcia, H. Wymeersch, E. G. Larsson, A. M. Haimovich, and M. Coulon, “Direct Localization for Massive MIMO,” IEEE Trans. Signal Process., vol. 65, no. 10, pp. 2475–2487, May 2017.

[10] H. Xiong, Z. Chen, B. Yang, and R. Ni, “TDOA localization algorithm with compensation of clock offset for wireless sensor networks,” China Commun., vol. 12, no. 10, pp. 193–201, Oct. 2015.

[11] M. Van Eeckhaute, T. Van der Vorst, A. Bourdoux, F. Quitin, P. De Doncker, and F. Horlin, “Low Complexity Iterative Localization of TimeMisaligned Terminals in Cellular Networks,” IEEE Trans. Veh. Technol., vol. 67, no. 11, pp. 10 730–10 739, Nov. 2018.

[12] X. Shao, C. You, W. Ma, X. Chen, and R. Zhang, “Target Sensing With Intelligent Reflecting Surface: Architecture and Performance,” IEEE J. Sel. Areas Commun., vol. 40, no. 7, pp. 2070–2084, Jul. 2022.

[13] A. Shahmansoori, G. E. Garcia, G. Destino, G. Seco-Granados, and H. Wymeersch, “Position and Orientation Estimation Through Millimeter-Wave MIMO in 5G Systems,” IEEE Trans. Wireless Commun., vol. 17, no. 3, pp. 1822–1835, Mar. 2018.

[14] B. Zhou, A. Liu, and V. Lau, “Successive Localization and Beamforming in 5G mmWave MIMO Communication Systems,” IEEE Trans. Signal Process., vol. 67, no. 6, pp. 1620–1635, Mar. 2019.

[15] M. Cui, L. Dai, R. Schober, and L. Hanzo, “Near-field wideband beamforming for extremely large antenna array,” arXiv preprint arXiv:2109.10054, 2021.

[16] C. Hu, L. Dai, T. Mir, Z. Gao, and J. Fang, “Super-Resolution Channel Estimation for MmWave Massive MIMO With Hybrid Precoding,” IEEE Trans. Veh. Technol., vol. 67, no. 9, pp. 8954–8958, Sep. 2018.

[17] N. Gonz´alez-Prelcic, H. Xie, J. Palacios, and T. Shimizu, “Wideband Channel Tracking and Hybrid Precoding for mmWave MIMO Systems,” IEEE Trans. Wireless Commun., vol. 20, no. 4, pp. 2161–2174, Apr.2021.

Thanks!